

After Treatment with Methylene Blue is Effective against Delayed Encephalopathy after Acute Carbon Monoxide Poisoning

Ningjun Zhao^{1,2}, Pengchong Liang³, Xiaoying Zhuo⁴, Chenglei Su^{1,2}, Xuemei Zong^{1,2}, Bingnan Guo^{1,2}, Dong Han^{1,2}, Xianliang Yan^{1,2}, Shuqun Hu^{1,2}, Quanguang Zhang⁵ and Xu Tie^{1,2}

¹Institute of Emergency and Rescue medicine, Xuzhou Medical University, Xuzhou, Jiangsu province, China, ²The Laboratory of Emergency Medicine, The Affiliated Hospital of Xuzhou Medical University, Xuzhou, Jiangsu province, China, ³Department of Emergency Medicine, Central Hospital of Baoji City, Baoji, Shanxi, China, ⁴School of Medical Imaging, Xuzhou Medical University, Xuzhou, Jiangsu province, China and ⁵Department of Neuroscience & Regenerative Medicine, Augusta University, Augusta, GA, USA

(Received 8 August 2017; Accepted 7 November 2017)

Abstract: Delayed encephalopathy after acute carbon monoxide (CO) poisoning (DEACMP) is the most severe and clinically intractable complication that occurs following acute CO poisoning. Unfortunately, the mechanism of DEACMP is still vague. Growing evidence indicates that delayed cerebral damage after CO poisoning is related to oxidative stress, abnormal neuro-inflammation, apoptosis and immune-mediated injury. Our recent report indicated that methylene blue (MB) may be a promising therapeutic agent in the prevention of neuronal cell death and cognitive deficits after transient global cerebral ischaemia (GCI). In this study, we aimed to investigate the potential of MB therapy to ameliorate the signs and symptoms of DEACMP. Rats were exposed to 1000 ppm CO for 40 min. in the first step; CO was then increased to 3000 ppm, which was maintained for another 20 min. The rats were implanted with 7-day release Alzet osmotic mini-pumps subcutaneously under the back skin, which provided MB at a dose of 0.5 mg/kg/day 1 hr after CO exposure. The results showed that MB significantly suppressed oxidative damage and expression of pro-inflammatory factors, including tumour necrosis factor- α and interleukin (IL)-1 β . MB treatment also suitably modulated mitochondrial fission and fusion, which is helpful in the preservation of mitochondrial function. Furthermore, MB dramatically attenuated apoptosis and neuronal death. Lastly, behavioural studies revealed that MB treatment preserved spatial learning and memory in the Barnes maze test. Our findings indicated that MB may have protective effects against DEACMP.

Carbon monoxide (CO) poisoning is one of the most common causes of poisoning in China [1], but the incidence of CO poisoning has decreased every year. A majority of poisoned patients recover from the acute stage of CO intoxication, and some patients exhibit a recurrence of neuropsychiatric symptoms after a latent period (usually 3–60 days) of normal or near normal neurological function, which is termed the lucid interval. These symptoms are referred to as Delayed encephalopathy after acute CO poisoning (DEACMP) [2,3]. The signs and symptoms of DEACMP include dementia, amnesic syndromes, Parkinsonism, aphasia, apraxia, tardive dyskinesia, cognitive deterioration, urinary incontinence, gait disturbance, mood disorders, memory deficits and personality changes [4]. Hyperbaric oxygen is a specific treatment for CO poisoning; however, approximately more than 50% of the survivors are still likely to develop DEACMP [5,6]. No specific

treatment is available for DEACMP [7], and approximately 25% of patients with DEACMP exhibit permanent neuropsychological deficits.

Previous studies showed that the demyelination and destruction of cerebral white matter (WM) induced by CO are considered to be the main pathological features of delayed encephalopathy. Choi *et al.* [8] reported that cerebral WM lesions were more often associated with neurological sequelae than globus pallidus lesions. Demyelination of the cerebral WM may present with axonal damage and gliosis. Nabeshima *et al.* [9] reported that delayed amnesia induced by CO exposure may result from delayed neuronal death in the hippocampal CA1 subfield. To date, the pathogenesis of delayed neuronal death in the hippocampal CA1 subfield has included the following: inflammation, mitochondrial oxidative stress, inhibition of mitochondrial function, lipid peroxidation, apoptosis and adaptive immunological responses [10–12].

Methylene blue (MB) has been used in clinics to treat various diseases for more than a century [13–15]. It has been reported that MB can reduce the formation of amyloid plaques and neurofibrillary tangles and can partially protect mitochondrial function [16,17]. Recent investigations have suggested that MB is capable of reducing reactive oxygen species (ROS) production by minimizing electron leakage from the

Author for correspondence: Xu Tie, Shuqun Hu, Institute of Emergency and Rescue medicine, Xuzhou Medical University, Xuzhou, 221002, Jiangsu province, China (e-mails xutie889@163.com (XT); hushuqun88@126.com (SH)).

and Quanguang Zhang, Department of Neuroscience & Regenerative Medicine, Augusta University, Augusta, 30912, GA, USA (e-mail qzhang@gru.edu).

Ningjun Zhao, Pengchong Liang and Xiaoying Zhuo have contributed equally to this work.

mitochondrial electron transport chain [18], promoting glucose uptake and increasing the intracellular ATP concentration and O₂ level, leading to a significant improvement in cell viability [19]. MB has also been shown to protect astrocytes from oxygen glucose deprivation (OGD) injury *in vitro* [20,21]. As a novel strategy, MB is receiving more attention due to its potential as an effective clinical option in the future and has recently been reported to possess neuroprotective functions [19]. Our previous study has investigated the potential beneficial effects of MB in a four-vessel occlusion (4VO) global cerebral ischaemia model (GCI) on adult male rats. MB was delivered at a dose of 0.5 mg/kg/day for 7 days, through a mini-pump implanted subcutaneously after GCI. It suggested that MB significantly improved cognitive deficits and attenuated neuronal cell death in the CA1 region following transient global cerebral ischaemia by rescuing ischaemia-induced decreases in cytochrome C oxidase (CCO) activity and ATP generation, preserving the depolarization of the mitochondrial membrane potential (MMP) and significantly reducing the increased numbers of ischaemia-induced TUNEL-positive cells in the CA1 region [22]. Therefore, we propose a new idea that MB may be a promising therapeutic agent targeting neuronal cell death and cognitive deficits following cerebral ischaemia, so then, MB may have protective effects against DEACMP.

In this study, we aim to put forward the first evidence that MB could provide dramatic therapeutic effects against DEACMP in rats. MB after treatments significantly reduced apoptosis and the inflammatory response decreased oxidative damage as well as improved cognitive function in a rat model of acute CO poisoning. The results suggest that MB is a promising drug for treating DEACMP. Our research provides the theoretical and technological basis for the clinical application of MB in patients with DEACMP.

Experimental Procedures

Animal models of CO poisoning. Male Sprague Dawley rats were purchased from the laboratory animal centre of Xuzhou Medical University. The rats were maintained on a 12-hr light/dark cycle. Water and food were provided *ad libitum*. All animal experiments were approved by the Institutional Animal Care and Use Committee of Xuzhou Medical University, and the methods were carried out in accordance with the approved guidelines (Assurance No. 2015-46, 2015-47). CO poisoning was performed according to the previously published protocol in a 7-L Plexiglas chamber [10,11,23–25]. Rats were put into the chamber and breathed 1000 ppm CO for 40 min. The CO concentration in the chamber was then increased to 3000 ppm, which was maintained 20 min. until the animals lost consciousness. They were then removed from the chamber to breathe room air and to regain consciousness.

Groups and drug administration. Rats were randomly divided into three groups: a normal group (sham; sham group), a CO + saline group (CO; CO group) and a CO + MB group (MB; CO + MB group). N = 10 in each group. Methylene blue (Fisher scientific, Pittsburgh, PA, USA) was administered via 7-day release Alzet osmotic mini-pumps (1007D, Durect Corporation, Cupertino, CA, USA) at 0.5 mg/kg/day. The mini-pumps were implanted subcutaneously under the upper back skin 1 hr after CO poisoning.

Histology examination. The animals were deeply anaesthetized with 2% pentobarbital sodium and underwent transcatheterial perfusion with 0.9% saline followed by cold 4% paraformaldehyde in 0.1 M phosphate buffer saline (PBS). Brains were removed and post-fixed in the same fixative overnight in paraformaldehyde and were cryoprotected with 30% sucrose in 0.1 M PB (pH 7.4) for 24–36 hr at 4°C until they sank. Coronal sections (25 µm) were then cut on a microtome (Leica RM2155, Nussloch, Germany) and collected through the entire dorsal hippocampus (~2.5–4.5 mm posterior from bregma, ~100 sections per brain) from animals killed at 6 days and 21 days after CO exposure or from animals in the sham group and every fifth section was collected and stained. For histological assessment, the sections were washed three times for 10 min. in PBS and then stained with 0.01% (w/v) cresyl violet for 10 min. Lastly, the sections underwent graded ethanol dehydration. An AxioVision4Ac microscope system (Carl Zeiss, Oberkochen, Germany) was used to examine the stained sections and to capture the images. For confocal staining, the sections were washed for 10 min. in PBS followed by two washes in 0.1% PBS–Triton X-100. After an incubation with blocking solutions containing 10% donkey serum for 1 hr at room temperature in PBS with 0.1% Triton X-100, sections were then incubated with mouse anti-NeuN monoclonal antibody (1:500; EMD Millipore, Billerica, MA, USA) overnight at 4°C. The sections were washed three times for 10 min. each with 0.1% Triton X-100 in PBS, followed by an incubation with Alexa Fluor 568 donkey antimouse antibody (1:500; Invitrogen, Grand Island, NY, USA) for 1 hr at room temperature. Next, sections were washed four times for 10 min. each with 0.1% PBS–Triton X-100 and were briefly washed with distilled water. Finally, the sections were mounted and cover-slipped in Vectashield mounting medium for fluorescence with 4', 6-diamidino-2-phenylindole (DAPI; H-1200; Vector Laboratories, Inc., Burlingame, CA, USA). Three to five sections from each animal (200 µm apart, approximately 1.5–3.3 mm posterior to bregma) were selected for confocal microscopy, and images were captured using a Zeiss LSM 510 META confocal laser microscope (Carl Zeiss) at 1024 × 1024 pixels as previously described [26]. The captured images were processed and analysed with the LSM 510 META software. The number of NeuN-positive CA1 neurons in the 250 µm length of the medial CA1 pyramidal cell layer was counted bilaterally in five sections per animal. Cell counts from the right and left hippocampus on each of the five sections were averaged to provide the mean value as reported before [27]. TUNEL staining was performed on free-floating coronal sections using the Click-iT[®] Plus TUNEL assay kit (Thermo Fisher Scientific) according to the manufacturer's instructions. Slides for a negative control were incubated with the label solution without terminal transferase for TUNEL. The quantification of the TUNEL-stained nuclei and the total nuclei was performed with Image-Pro software and was presented as a percentage of the total number of nuclei in the field as described previously [28].

Double/triple immunofluorescence staining. Brain tissues were embedded in optimal cutting temperature (OCT) compound, and frozen coronal sections (25 µm) were cut through the dorsal hippocampus. Thereafter, the sections were washed four times for 10 min. each with 0.1% PBS–Triton X-100 and then were briefly washed with distilled water. The coronal sections were incubated with 10% normal donkey serum for 1 hr at room temperature in PBS containing 0.1% Triton X-100, followed by an incubation with appropriate primary antibodies overnight at 4°C in the same buffer. The following primary antibodies were used in different combinations: anti-NeuN, OPA1, DRP1, 4-HNE, P-H2AX. After the primary antibody incubation, the sections were washed four times for 10 min. each at room temperature, followed by an incubation with Alexa Fluor 594/647 donkey antimouse/rabbit, Alexa Fluor 488 donkey anti-rabbit/mouse, and Alexa Fluor 568 donkey anti-goat secondary antibody (1:500; Invitrogen Corporation, Carlsbad, CA, USA) for 1 hr at room

temperature. The sections were then washed four times with PBS containing 0.1% Triton X-100 for 10 min. each, followed three times for 5 min. each with PBS and were then briefly washed with water, and then, the sections were mounted and cover-slipped in Vectashield mounting medium for fluorescence with DAPI (H-1200; Vector Laboratories). Three to five sections from each animal (200 μ m apart, approximately 1.5–3.3 mm posterior to bregma) were selected for confocal microscopy.

Confocal microscopy and image analysis. All of the double- and triple-labelled images were captured on a Zeiss LSM 510 META confocal laser microscope (Carl Zeiss) using either a 5 \times or a 40 \times oil immersion Neofluar objective (NA, 1.3) with the image size set at 1024 \times 1024 pixels. The following excitation lasers/emission filter settings were used for various chromophores: the Argon/2 laser was used for Alexa Fluor 488, with an excitation maximum at 490 nm and an emission in the range of 505–530 nm; the HeNe1 laser was used for Alexa Fluor 594 with an excitation maximum at 543 nm and an emission in the range of 568–615 nm; and the HeNe2 laser was used for Alexa Fluor 647 with an excitation maximum at 633 nm and an emission in the range of 650–800 nm. The captured images were processed and analysed using LSM 510 META imaging software. Data were calculated as the mean \pm S.E. from five independent animals per group.

Tissue preparation and Western blot analysis. All animals were killed under deep anaesthesia at the time-points stated in the experiments. Whole brains were quickly removed, and the hippocampal CA1 regions were rapidly microdissected from both sides of the hippocampal fissure and were immediately frozen in liquid nitrogen. The samples were homogenized as previously described [29]. Briefly, tissues were homogenized in ice-cold homogenization medium containing 50 mM HEPES (pH 7.4), 150 mM NaCl, 12 mM β -glycerophosphate, 3 mM dithiothreitol (DTT), 2 mM sodium orthovanadate (Na_3VO_4), 1 mM EGTA, 1 mM NaF, 1 mM phenylmethylsulfonyl fluoride (PMSF), 1% Triton X-100 and inhibitors of proteases and enzymes (0.5 mM PMSF, 10 μ g/mL each of aprotinin, leupeptin and pepstatin A) with a Teflon-glass homogenizer. Then, samples were centrifuged at 800 \times g for 20 min. to yield a cytoplasmic supernatant, and the deposit was sonicated with ice-cold buffer A followed by centrifugation at 17,000 \times g for 20 min. to obtain the mitochondrial supernatant; supernatants were collected and stored at -80°C until use. The protein concentrations were determined with a Lowry protein assay kit with bovine serum albumin as a standard.

For Western blotting analysis as previously described [29], the samples were mixed with loading buffer and boiled for 5 min. An aliquot of 20–50 μ g of protein was separated with 4–20% sodium dodecyl sulphate–polyacrylamide gel electrophoresis. Proteins were transferred to a PVDF membrane, blocked for 3 hr and incubated with a primary antibody against Bax1 (Proteintech, Rosemont, IL, USA), Bcl2 (Proteintech), SOD2 (Proteintech), GAPDH (Proteintech), MFN1 (Millipore), OPA1 (Invitrogen, NY, USA), mitochondrial elongation factor (MIEF; Millipore), mitochondrial fission factor (MFF; Millipore), DRP1 (Santa Cruz Biotechnology, Santa Cruz, CA, USA), COXIV (concentration of 1:50–500; Santa Cruz Biotechnology) at 4 $^\circ\text{C}$ overnight. HRP (horseradish peroxidase)-labelled GAPDH (1:4000; Proteintech) was used as a loading control for the total cell protein. The membrane was then washed with T-TBS to remove unbound antibodies, followed by an incubation with a secondary bio-conjugated goat anti-rabbit/mouse IgG for 1–2 hr at room temperature. The membrane was then washed with T-TBS to remove unbound antibody, followed by an incubation with a third Avidin-HRP antibody for 1–2 hr at room temperature (HRP-labelled GAPDH did not need a secondary or third antibody). Membranes were then washed three times for 5 min. each with T-TBS and were briefly washed with distilled water. The membranes were immersed in the optimized 4IPBA-ECL solution

(100 mM Tris/HCl pH 8.8, 1.25 mM luminol, 2 mM 4IPBA, 5.3 mM hydrogen peroxide) and 30% hydrogen peroxide [30]. Bound proteins were visualized using a Canon camera (Canon USA, Inc., Melville, NY, USA) and the camera control pro 2 software. Semi-quantitative analyses of the bands were performed with ImageJ software (version 1.30 v; Wayne Rasband, NIH, Bethesda, Maryland, USA). To quantify hippocampal protein abundance, band densities were corrected for variations in loading and were normalized to the corresponding band densities for total protein signals, and the indicated total proteins were expressed relative to GAPDH or COX IV expression. Normalized numerical means were then expressed as relative intensities of the corresponding values for control (sham-operated) animals. A mean \pm S.E. was calculated from the data from all of the animals for graphical presentations and statistical comparisons.

Mitochondrial cytochrome C oxidase activity. Cytochrome C oxidase is a part of the CCO subunit complex, which is located in the inner membrane of the mitochondria and is the terminal electron acceptor in the electron transfer chain; the CCO subunit complex converts molecular oxygen to water and facilitates the synthesis of ATP. The hippocampal CA1 regions from rats 6 days after CO poisoning were homogenized using the aforementioned method for brain tissue preparation. The crude mitochondrial fractions were collected by centrifuging the homogenates at 15,000 \times g for 15 min. at 4 $^\circ\text{C}$. CCO activity in the mitochondrial fractions was assessed using an activity assay kit (ab109911; Abcam, Inc., Cambridge, MA, USA) according to the instructions of the manufacturer. The ability of CCO to oxidize fully reduced ferrocytochrome C to ferricytochrome C was measured using spectrophotometry. The absorbance of oxidized ferricytochrome C was measured as a loss of absorbance at 550 nm (Microplate Spectrophotometer; Bio-Rad Benchmark Plus, Hercules, California, USA) in a 96-well plate reader. The presented value was calculated by the absorbance divided by the mitochondrial lysate protein levels.

Pro-inflammatory cytokines assay. The levels of pro-inflammatory cytokines in each group were quantified with the indirect enzyme-linked immunosorbent assay (ELISA) technique [31]. Briefly, rats were killed under anaesthesia at the indicated time-points. Whole brains were removed, and the hippocampal CA1 regions 6 days after CO poisoning were microdissected from both sides of the hippocampal tissue and immediately frozen in dry ice. Protein samples were extracted as above tissue preparation method. Samples were diluted to 50 μ L containing the same amount of protein using bicarbonate/carbonate coating buffer (Sigma-Aldrich, St. Louis, MO, USA). The dilutions were then loaded into the ELISA microplate (Corning, NY, USA), sealed and incubated overnight at 4 $^\circ\text{C}$. The plate wells were washed three times, and the remaining protein-binding sites in the coated wells were blocked by adding 200 μ L of blocking buffer (1% BSA in PBS, 0.3% solution of H_2O_2) for 2 hr at room temperature. Afterwards, 50 μ L of monospecific antibodies was added and the plate was incubated for 2 hr at 37 $^\circ\text{C}$. The plate wells were then washed three times and incubated with HRP-conjugated secondary antibodies for 1 hr at room temperature, followed by another three washes. Finally, the plate was developed by adding 3, 3', 5, 5'-tetramethylbenzidine (TMB) solution (Thermo fisher) to the wells and incubating the plate for 30 min. at room temperature and the reaction was stopped with 50 μ L of sulphuric acid. The optical density was read at 450 nm on a spectrophotometer (Bio-Rad), and values were calculated and expressed as percentage changes *versus* the control group.

Barnes maze. The Barnes maze test, which is widely used to assess hippocampal-dependent spatial learning and memory [32,33], was utilized as previously described [22]. The Plexiglas apparatus is a 122 cm diameter circular platform on a 1.0 m stand with 18 evenly spaced 10-cm diameter holes around the circumference with a black box (escape box, 20 \times 15 \times 12 cm) placed underneath one of the

holes. Several visual cues were pasted to the black walls surrounded the platform to facilitate the use of spatial cues by the rat. Testing was performed in a darkened room with a bright flood incandescent light (500 W, 1000 lux) shining down on the maze surface. Rats were also exposed to noxious auditory stimuli with the use of digital metronome software and two computer speakers facing the platform.

Prior to the first trial, animals were subjected to a habituation trial by gently placing the rat in the middle of the platform under an opaque Plexiglas tube (diameter = 27 cm, height = 23 cm) and allowing the rat to enter the escape box for 1 min before being returned to its home cage. On day 18 after CO poisoning, 3 days of training trials were performed. The rat was then placed in the centre of the maze, the tube was slowly raised, and the rat was allowed 300 sec. to locate the escape box. If the rat did not find and enter the escape box within the time limit, it was guided to the box and allowed 15 sec. inside before being returned to its home cage. On the subsequent 2 days, the same procedure was followed and each rat was tested in one trial per day. The time to enter the target hole was recorded. The probe trial was performed on day 21 after GCI. The platform and escape box were cleaned with 70% ethanol between each test. Video recordings were made using a FUJINON Lens, Vari-focal, 2.7–13.5 mm (FUJIFILM Corporation, Valhalla, NY, USA). The primary latency and the time spent in quadrants were quantified using ANY-maze video tracking software (Stoelting Co., Wood Dale, IL, USA).

Statistical analysis. All values are presented as the means \pm S.E.s. Statistical analyses included one-way or two-way analysis of variance (ANOVA) with SigmaStat 3.0 software (SPSS, Inc., Chicago, IL, USA), followed by Student–Newman–Keuls *post hoc* tests (for all pairwise comparisons) or Dunnett's *post hoc* tests (for multiple comparisons *versus* a control) or Student's *t*-test (for the comparison of only two groups). A *p* value of <0.05 was considered to be statistically significant.

Results

MB suppressed pro-inflammatory cytokine production post-CO poisoning in the hippocampal CA1 region.

Because DEACMP is associated with an increased inflammatory response in the early stage of CO poisoning, we examined the effect of MB on inflammation in hippocampal CA1 neurons with highly sensitive ELISA assays. The expression of the typical pro-inflammatory factors IL-1 β and TNF- α was subsequently examined 6 days after CO poisoning. IL-1 β and TNF- α secretion was significantly higher in the CO group (the second panel in fig. 1A,B). In contrast, after treatment with MB dramatically suppressed the expression of IL-1 β (fig. 1A) and TNF- α (fig. 1B) to near control levels. All data were analysed and expressed as fold changes *versus* the sham group in diagram forms.

MB enhanced mitochondrial oxidative phosphorylation level and the antioxidant capacity to protect mitochondrial function.

Cytoplasmic cytochrome *C* is released from the mitochondria after mitochondrial dysfunction, and CCO activity was subsequently tested to evaluate mitochondrial oxidative phosphorylation levels. Data showed that CCO activity decreased noticeably in the CO group (the second panel in fig. 1C); however, MB after treatment dramatically boosted the activity of CCO, revealing an attenuation of mitochondrial function

with MB treatment. Western blotting analysis of the representative antioxidant enzyme SOD2 6 days after CO exposure indicated that levels of SOD2 were remarkably up-regulated after MB treatment compared to levels in the CO group (fig. 1D), demonstrating the enhancement of antioxidant capacity with MB treatment, consistent with CCO.

MB suppressed hypoxia-induced mitochondrial dysfunction after CO exposure and inhibited the apoptotic pathway.

Mitochondria are the major cellular energy source, and mitochondrial dysfunction, which is characterized by a series of pathological events, including Bax-involved megaspore formation within the mitochondrial outer membrane, will directly initiate cell apoptosis. We tested the effect of MB on these mitochondrial dysfunction indices to investigate whether MB could attenuate CO poisoning-induced mitochondrial abnormalities in the hippocampal CA1 region. We examined the expression of Bax, an apoptosis regulator involved in the opening of the outer mitochondrial membrane, and Bcl-2, an anti-apoptosis protein, by Western blotting. The ratio of Bax and Bcl-2 expression is presented in diagram form (fig. 2A–D). Data showed that increased Bax activation and decreased Bcl-2 expression were induced 6 days after CO exposure, and these alterations were reversed with MB treatment, leading to a subsequent decline in the Bax to Bcl-2 ratio. To analyse CO poisoning-induced apoptotic cell death of hippocampal CA1 neurons, coronal brain sections were also subjected to TUNEL staining. As shown in fig. 2E,F, in the CO group, most of the hippocampal CA1 neurons were positive for TUNEL. However, quantitative analyses indicated that the number of TUNEL-positive cells in the pyramidal cell layer was significantly attenuated in the MB after treatment animals compared with the CO animals. These data clearly indicated the ability of MB to inhibit the intrinsic apoptotic pathway after CO exposure.

MB attenuated hypoxic oxidative damage after CO exposure and increased anti-oxidant capacity in the hippocampal CA1 region.

Reactive oxygen species play a critical role in neuronal damage, so evidence of the oxidative damage of basic biological molecules such as lipid peroxidation, histone peroxidation and DNA damage induced by ROS accumulation was analysed during the early stage of CO poisoning by fluorescent staining using anti-HNE and anti-P-H2AX antibodies (fig. 3). Representative confocal images demonstrated that these oxidative markers were elevated in the CO group compared with the sham group, and the staining intensity for markers was attenuated by MB treatment. This result suggested that MB increased the anti-oxidant capacity in hippocampal CA1 neurons.

MB inhibited the expression of mitochondrial fission proteins in the CA1 region at an early stage of DEACMP.

The mitochondrial targeting fission proteins dynamin-related protein 1 (DRP1), MFF and MIEF are involved in the mitochondrial fission process, which facilitates mitochondrial

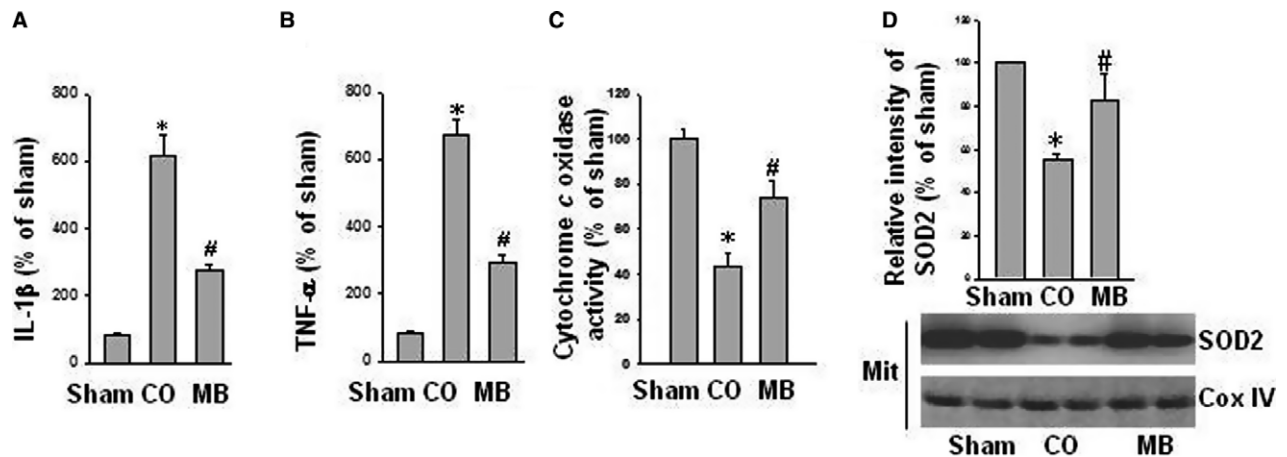


Fig. 1. Methylene blue (MB) inhibits pro-inflammatory cytokines production and enhances mitochondrial oxidative phosphorylation level, antioxidant capacity. (A,B) Levels of representative pro-inflammatory cytokines interleukin-1 β and TNF- α 6 days after carbon monoxide (CO) poisoning were detected by enzyme-linked immunosorbent assay assays, and CO poisoning-induced up-regulation of these pro-inflammatory cytokines was significantly suppressed by MB. (C) Cytoplasmic cytochrome *C* content is released from mitochondria after mitochondrial dysfunction, and cytochrome *C* oxidase activity was subsequently tested to evaluate mitochondrial oxidative phosphorylation level, revealing attenuation of MB treatment on mitochondrial function. (D) Western blotting analysis of representative antioxidant enzymes SOD2, respectively, 6 days after CO poisoning. Consistent with (C), levels of SOD2 (mean \pm S.E., $n = 5$ animals per group) were remarkably up-regulated after MB treatment compared with the CO group, showing apparent enhancement of MB on antioxidant capacity. Data are presented as mean \pm S.E., $n = 5$ animals per group. * $p < 0.05$ versus sham, # $p < 0.05$ versus CO.

fragmentation and mitophagy. We investigated the effect of MB on the expression of these mitochondrial fission proteins via Western blotting analysis and confocal imaging. The results indicated that mitochondrial fission proteins were remarkably elevated in the CO group compared with the sham group, and mitochondrial fission protein expression was significantly suppressed by MB treatment (figs 4 and 6A).

MB increased the expression of mitochondrial fusion proteins in the hippocampal CA1 region at an early stage of DEACMP.

Dynammin-like 120 kDa protein (OPA1) is a critical mitochondrial targeting fusion protein that regulates mitochondrial fusion and cristae structure in the inner mitochondrial membrane, and mitofusin 1 (MFN1) is a mediator of mitochondrial fusion. The expression of these proteins was investigated by Western blotting (fig. 5) and confocal analysis (fig. 6B). As shown in fig. 5A,B, MFN1 and OPA1 expression was drastically decreased in the CO group compared with the sham group, and the expression of these proteins was remarkably elevated in the MB group. The results were quantified as relative intensity in diagram form with values expressed as fold changes *versus* the sham group. To further verify the former result, confocal analysis was carried out with OPA1 fluorescent staining of hippocampal CA1 neurons. Corresponding to Western blot results, confocal images showed that the expression of fusion proteins within mitochondria was remarkably lower in the CO group, and significantly elevated after MB treatment, indicating that mitochondrial integrity was preserved by MB at an early stage of DEACMP progression.

MB after treatment significantly decreased delayed neuronal cell death in the rat hippocampal CA1 region induced by CO poisoning.

We first evaluated the neuroprotective effects of MB after treatment against delayed neuronal cell death induced by CO poisoning. The evaluation of cresyl violet staining and NeuN staining revealed a loss of local neurons in the hippocampal CA1 region of the CO group compared with sham animals (the second panel in fig. 7A–C). As revealed via cresyl violet staining, cells in the hippocampal CA1 pyramidal cell layer showed unequivocal signs of condensed, pyknotic and shrunken nuclei 21 days after CO exposure. In contrast, cresyl violet/NeuN staining and cell quantification showed that MB after treatment significantly increased the number of surviving neurons in the hippocampal CA1 region following CO exposure (the third panel in fig. 7A–C), in comparison with the CO group. These results verify the novel neuroprotective effects of MB after treatment against delayed neuronal cell death in the hippocampal CA1 region following CO exposure.

MB after treatment significantly attenuated spatial learning and memory deficits induced by CO poisoning.

It has been reported that ischaemic rats showed exploratory behaviour changes and cognitive neurobehavioural deficits [34–37]. The hippocampus plays an important role in the processing of spatial locations, especially within the CA1 region [38]. The Barnes maze test was used to assess hippocampal-dependent spatial learning and memory [32,33]. To document whether the neuroprotective effects of MB that reduced neuronal cell death also led to functional improvement, we then evaluated spatial learning and memory ability in the Barnes maze. All animals were subjected to training trials at 18, 19

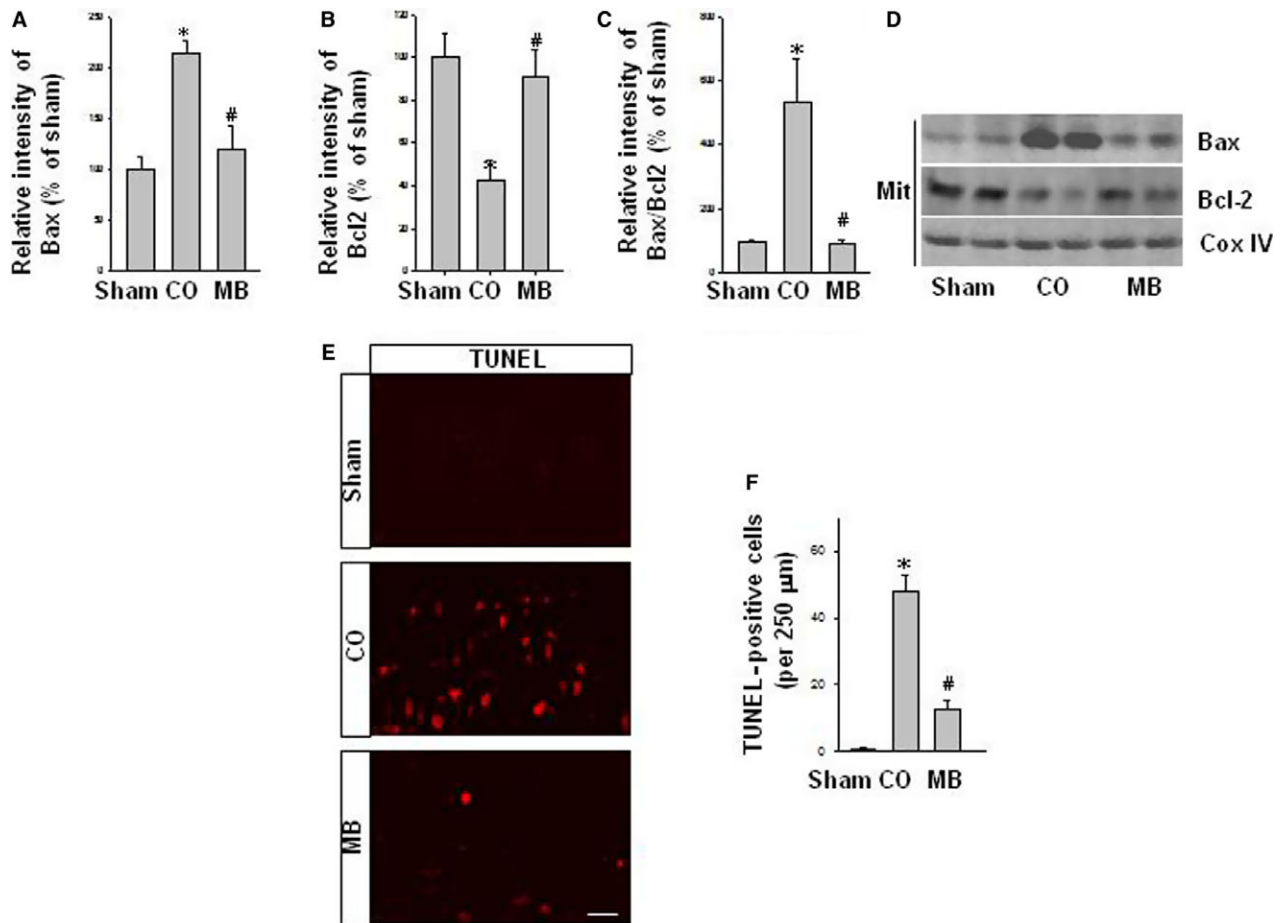


Fig. 2. Methylene blue (MB) attenuates mitochondrial dysfunction as determined by inhibited mitochondrial megaspores formation and alleviates neuron apoptosis 6 days after carbon monoxide (CO) poisoning. (A–D) The opening of outer mitochondrial membrane exerts to be anti-apoptotic. Ratio of Bax to Bcl-2 was expressed in a diagram form. Values are means \pm S.E.M. of determinations from each group. * $p < 0.05$ versus sham, # $p < 0.05$ versus CO. (E,F) TUNEL assay was performed by confocal analysis. Aggravated TUNEL was observed after mitochondrial dysfunction, while reversed by MB, indicating efficacious anti-apoptosis of MB treatment at early stage of CO poisoning. Positive cell numbers per 250 μm in each confocal picture were counted and presented. Values are means \pm S.E.M. of determinations from each group. (Magnification: 20 \times ; scale bar: 50 μm). Data are presented as mean \pm S.E., $n = 5$ animals per group. * $p < 0.05$ versus sham, # $p < 0.05$ versus CO.

and 20 days after CO exposure, and the probe trials were performed on day 21 after CO exposure. As shown in fig. 8A,B, the animals in the CO group took more time to find the black escape box compared with the sham rats. MB-treated animals showed significantly decreased escape latencies to find the escape box during the last training trials. In the probe test on day 21 after GCI, the animals in the CO group spent significantly shorter times in the target quadrant zone than the MB-treated animals and the sham animals (fig. 8C,D). For this reason, treatment with MB has the ability to significantly attenuate learning and memory impairment after the injury of hippocampal CA1 neurons induced by CO poisoning.

Discussion

It is well known that CO is colourless, odourless and tasteless and is formed by the incomplete combustion of carbon-containing substances. CO passes into the bloodstream via alveoli

after being inhaled into the upper respiratory tract. CO combines with haemoglobin to immediately form carboxyhaemoglobin (COHb); haemoglobin loses the capacity to carry oxygen, causing tissue hypoxia and poisoning. The tantalizing issue for clinicians is that a major fraction of acute poisoning patients recover from the acute stage of CO intoxication, and some patients exhibit a recurrence of neuropsychiatric symptoms after a latency period, defined as DEACMP. Compelling evidence has shown that the main pathological mechanism of DEACMP may be delayed neuronal death in the hippocampal CA1 subfield [9]. The pathogenesis of delayed neuronal death in the hippocampal CA1 subfield has been shown to include: inflammation, mitochondrial oxidative stress, inhibition of mitochondrial function, lipid peroxidation, apoptosis and adaptive immunological responses [10–12].

In the present study, we report that methylene blue treatment initiated 1 hr after CO exposure decreased pro-inflammatory cytokine levels, suppressed oxidative damage, preserved

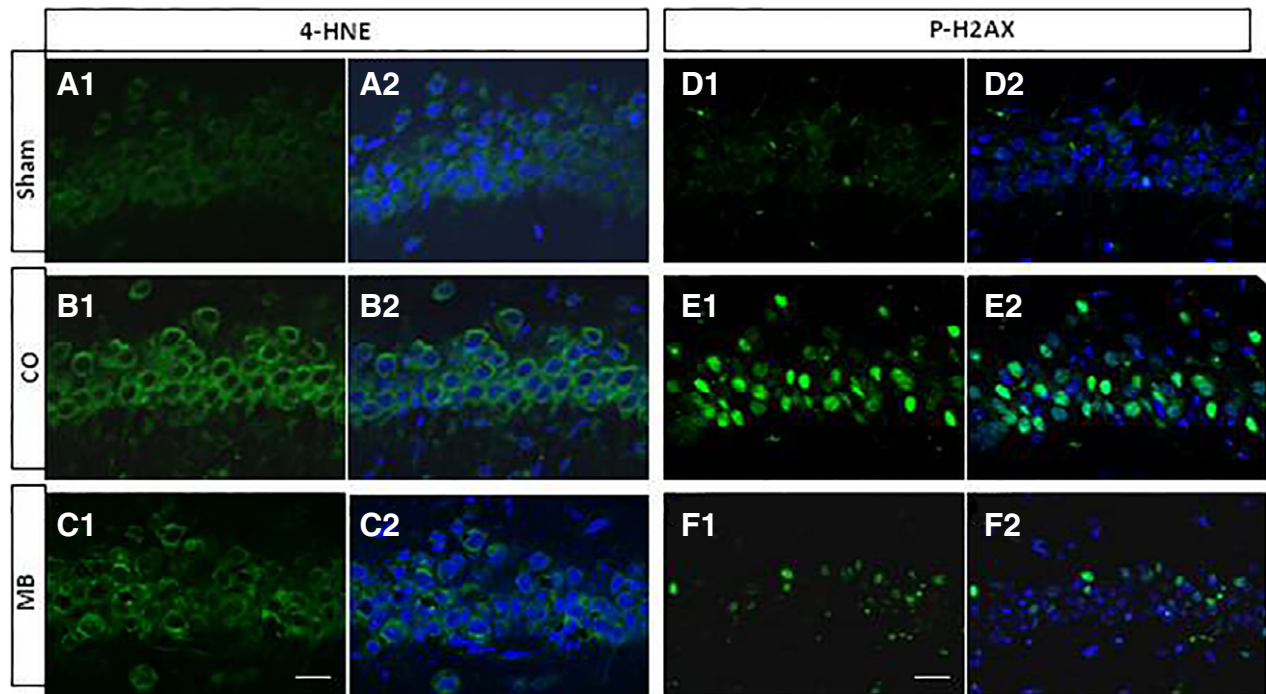


Fig. 3. Methylene blue (MB) alleviates oxidative lesions to basic biological components 6 days after carbon monoxide (CO) poisoning. Representative confocal pictures of basic biological components oxidation were taken from medial CA1 region 6 days after CO poisoning. (a–c) show effect of MB on lipid peroxidation damage marked by 4-HNE. (d–f) show remarkable attenuation of MB on CO poisoning-induced evident histone oxidative damage marked by P-H2AX. Note that MB strongly decreased oxidative damage to basic biological components at the early stage of CO poisoning. (Magnification: 20 \times ; scale bar: 50 μ m). Data are presented as mean \pm S.E., n = 5 animals per group.

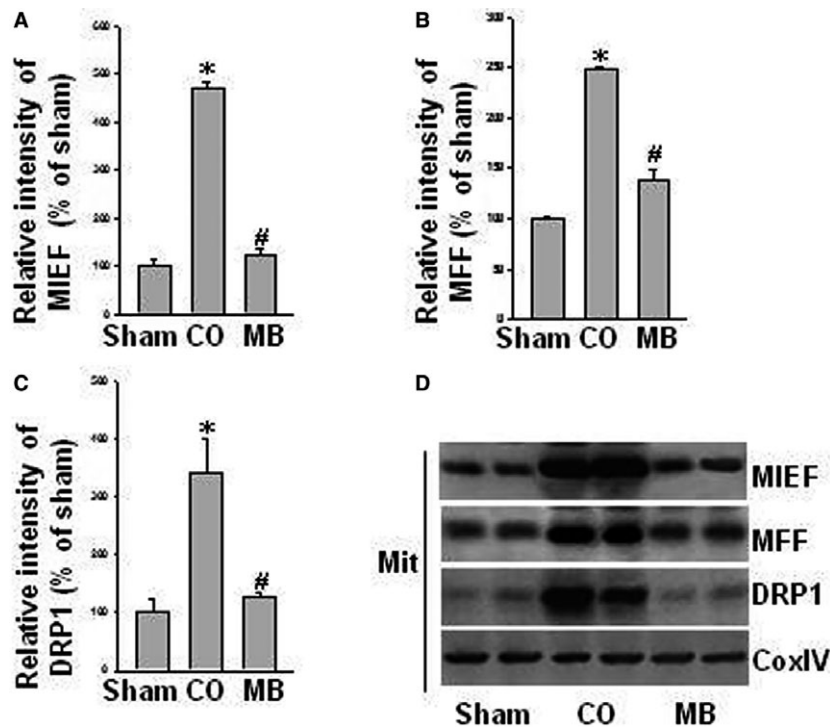


Fig. 4. Effects of methylene blue on mitochondrial targeting fission proteins. (A–D) Western blotting analysis of mitochondrial fission proteins Mff, MIEF as well as DRP1, which exert functions in mediating mitochondrial fission process, was performed with hippocampal CA1 proteins. Data are presented as mean \pm S.E., n = 5 per group. * p < 0.05 versus sham, # p < 0.05 versus carbon monoxide.

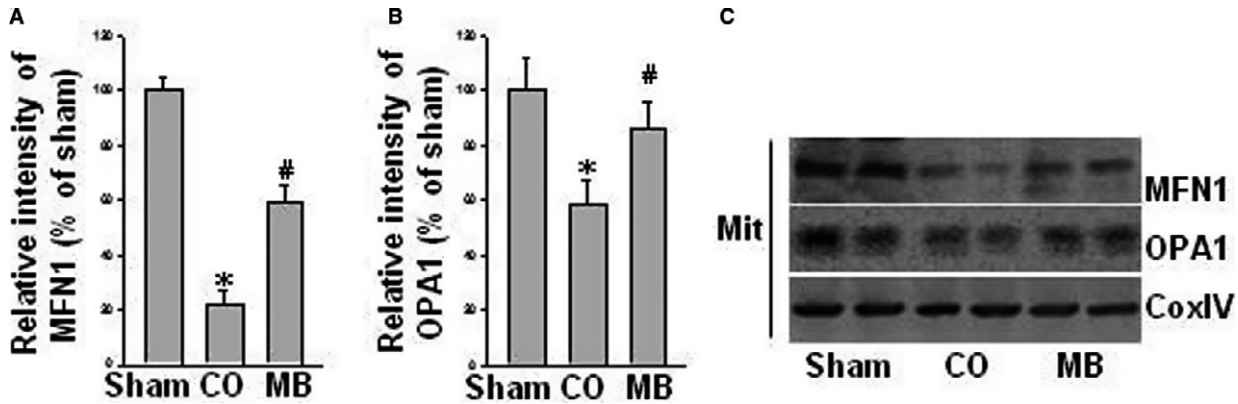


Fig. 5. Effects of methylene blue on mitochondrial targeting fusion proteins. (A–C) Western blotting analysis of mitochondrial fusion proteins MFN1 and OPA1, which exert functions in mediating mitochondrial fusion process, was performed with hippocampal CA1 proteins. Data are presented as mean \pm S.E., $n = 5$ per group. * $p < 0.05$ versus sham, # $p < 0.05$ versus carbon monoxide.

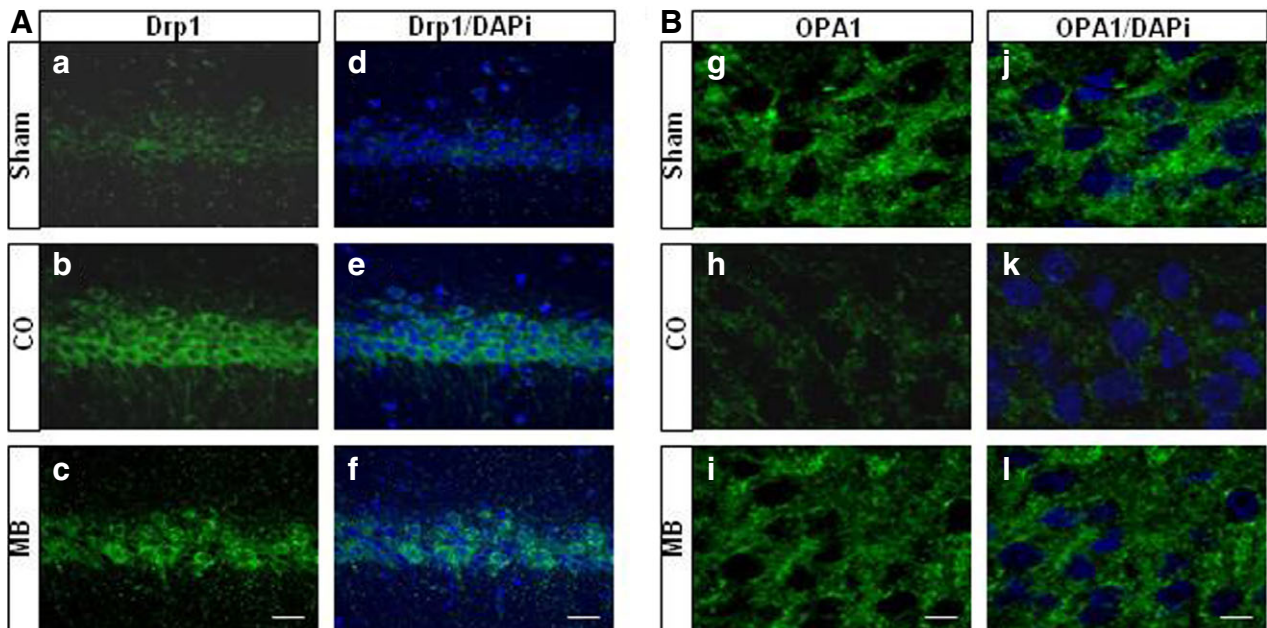


Fig. 6. Effects of methylene blue (MB) on mitochondrial targeting fission and fusion proteins. Representative confocal pictures of DRP1 and OPA1 were taken from medial CA1 region 6 days after carbon monoxide poisoning. (a–f) show obvious inhibition effect of MB on expression of DRP1 (mitochondrial targeting fission). (Magnification: 20 \times ; scale bar: 50 μ m). (g–l) reveal obvious enhancement effect of MB on expression of OPA1 (mitochondrial targeting fusion). (Magnification: 40 \times ; scale bar: 25 μ m).

mitochondrial function, reduced neuronal apoptosis in the hippocampus and alleviated cognitive impairments in a rat model of severe CO poisoning. We therefore suggest that MB is neuroprotective against DEACMP.

During ischaemia and reperfusion, the mitochondrial electron respiratory chain is the main cellular source of free radical generation. ROS produced by hypoxic cells play a pivotal role in brain injury. Similarly, a source of the free radicals is produced during tissue hypoxia after CO poisoning [24]. ROS leads to the initiation of lipid peroxidation, which in turn causes the destruction of the cell membrane [10,23]. Cell membrane damage can cause neuropathological effects that contribute to the delayed development of neurological sequelae [11]. Moreover, the vicious cycle of neuro-inflammation

results in prolonged inflammation that exacerbates the original injury induced by ischaemia/reperfusion after global cerebral ischaemia [39]. Inflammation induced by CO exposure is also critical in the delayed development of neurological sequelae after CO poisoning [11,25]. Consistent with the results of previous studies, the current result shows that MB was effective in the alleviation of inflammation by inhibiting the expression of pro-inflammatory cytokines, such as IL-1 β and TNF- α . The elevated expression of typical anti-oxidant enzymes, such as SOD2, was also detected after MB treatment via Western blotting analysis.

We examined Bax and Bcl-2 expression as well as their ratio. Our data indicated that elevated Bax activation and decreased Bcl-2 expression were induced 6 days after CO

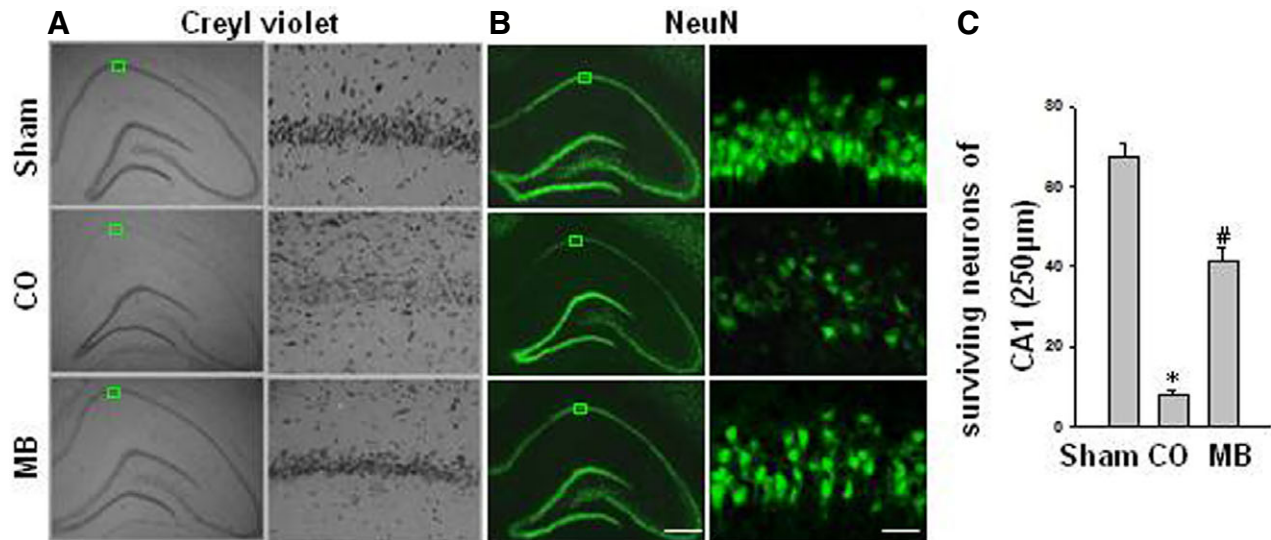


Fig. 7. Neuroprotective effects of methylene blue (MB) in the hippocampal CA1 region in Adult SD rats at day 21 following carbon monoxide (CO) poisoning. (A,B) Representative photomicrographs of hippocampal Cresyl violet and NeuN staining in sham animals and in animals who were 21 days post-CO poisoning, either with (MB) or without MB treatment. NeuN-positive CA1 pyramidal cells showing intact and round nuclei after CO poisoning were counted as surviving cells. (C) Quantitative summary of data (mean \pm S.E., $n = 5$ animals per group) showed the number of surviving neurons per 250 μm length of medial CA1. (Magnification: Creyl violet = 4 \times , 10 \times ; NeuN = 4 \times , 20 \times ; scale bar: 50 μm .) * $p < 0.05$ versus sham, # $p < 0.05$ versus CO.

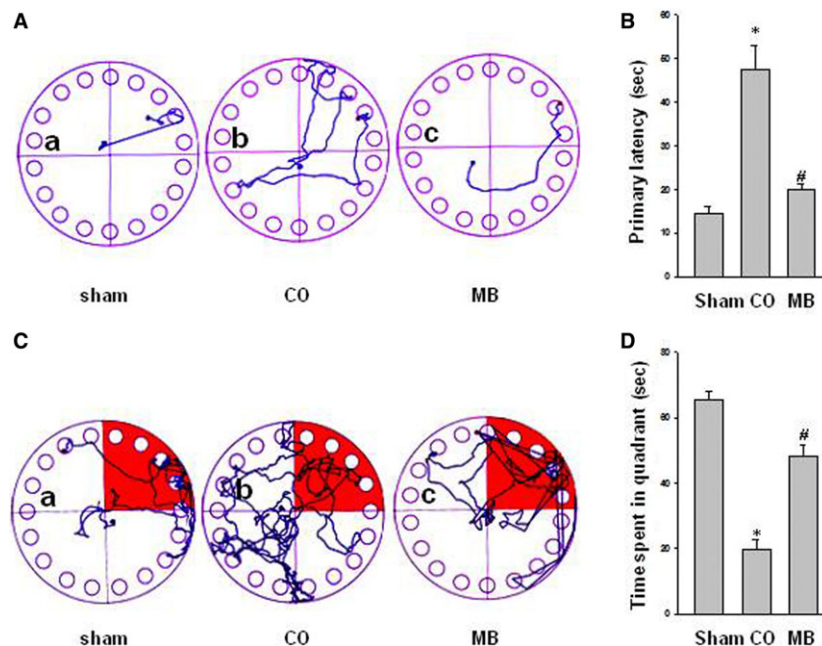


Fig. 8. Methylene blue (MB) significantly attenuated learning and memory deficits of delayed encephalopathy after acute carbon monoxide (CO) poisoning. (A, B) The Barnes maze task was performed to test the spatial learning ability of animals. This ability was measured by the latency to find the black escape box at day 20 after CO poisoning. (C,D) A probe test was performed at day 21 after CO poisoning by removing the escape box and recording the total time spent exploring the quadrant where the escape box had been located. The representative tracks in the quadrant zone are shown. Data are presented as mean \pm S.E., $n = 5$ per group. * $p < 0.05$ versus sham, # $p < 0.05$ versus CO.

exposure. MB treatment caused the Bax to Bcl-2 ratio to decline. To analyse CO poisoning-induced apoptotic cell death of hippocampal CA1 neurons, evidence of oxidative damage to basic biological molecules such as lipid peroxidation, histone peroxidation and DNA damage induced by ROS

accumulation was analysed. MB treatment alleviated oxidative damage in hippocampal CA1 neurons. TUNEL staining indicated that the number of TUNEL-positive cells in the pyramidal cell layer was significantly attenuated in the MB after treatment animals compared with the CO animals. These

data clearly indicate the ability of MB to inhibit the intrinsic apoptotic pathway and to attenuate CO poisoning-induced mitochondrial abnormalities and neuronal cell death in the hippocampal CA1 region.

Now that mitochondrial dysfunction has been shown to play a key role in the delayed neurological sequelae associated with neurodegeneration [40], further studies are needed to verify whether and how MB treatment preserves mitochondrial function. According to the endosymbiosis theory, mitochondria have been observed not to exist in a fixed position, but are highly dynamic with constant alterations between fission and fusion statuses, which is considered to be a representative event in many neurodegenerative disorders [41]. Fission proteins such as DRP1, MIEF and MFF regulate mitochondrial fission, break down mitochondrial structure and facilitate mitophagy, leading to mitochondrial fragmentation and cytochrome *C* release into the cytoplasm. In contrast, fusion proteins such as by OPA1 and MFN1 have been implicated in mitochondrial structure preservation, regulating mitochondrial morphology by balancing the processes of fission and fusion. The mechanism of mitochondrial structure preservation has been widely reported to be associated with the balance of mitochondrial fission and fusion protein expression [42]. Mitochondrial fission, a division event that fragments mitochondria into small particles in response to the initiation of cellular apoptosis, is co-ordinated by DRP1. Multiple mitochondrial localized adaptor proteins that have been identified in mammals, such as MFF and MIEF, can recruit DRP1 to mitochondria [43]. Based on the need for various mitochondrial functions in specific tissues, mitochondria need to change their morphology via fusion [44]. Fusion is evolutionarily conserved from yeast to human beings and is fundamental to eukaryotic life. The elimination of fusion has been demonstrated to result in embryonic lethality in mouse models [45]. Two mitochondria are needed for fusion initiation. Once close contact is established, the fusion process will start with outer-mitochondrial membrane (OMM) fusion via dynamin-related OMM proteins MFN1 and MFN2, followed by OPA1-mediated fusion. In the current study, the fusion proteins levels were significantly elevated, while the fission proteins were suppressed at relatively low levels by MB treatment, consistent with previous findings. Consequently, the balance of these proteins that exert wholly opposite functions is crucial for mitochondrial structure integrity and neuronal plasticity.

Mitochondrial dysfunction can be fatal to hippocampal neurons that are responsible for spatial learning and memory functions [41]. Deficits in cognitive functioning are a well-known co-morbidity in DEACMP. Using the Barnes maze, our studies revealed that MB after treatment significantly attenuated functional impairments in spatial learning and memory following CO poisoning.

Conclusion

In conclusion, the results of the current study demonstrate that methylene blue after treatment initiated 1 hr after CO exposure

could attenuate pro-inflammatory cytokines levels, suppress oxidative damage, preserve mitochondrial function and reduce neuronal apoptosis in a rat model of DEACMP. MB after treatment has the ability to attenuate hippocampal neuronal loss and improve some behavioural outcome with respect to spatial learning memory of DEACMP. Therefore, MB after treatment may have protective effects against DEACMP. However, as the precise mechanism of DEACMP remains unclear, further study is warranted prior to progressing to the clinical arena.

Acknowledgements

This research was supported by the National Natural Science Foundation of China (81271267), Jiangsu social development or Natural Science Foundation (BE2016645, BK20161153, BE2017641, BK20141136), Xuzhou Natural Science Foundation (KC15J0060, KC15SX009), Jiangsu Educational Science Foundation (16621628, KJS1410, 17KJB320021), Jiangsu Provincial Commission of Health and Family Planning, Genera Programs (H201527), The Project of Invigoration Healthcare through Science, Technology and Education and Jiangsu Provincial Medical Youth Talent (QNRC2016797).

Competing financial interests

The authors declare no competing financial interests.

References

- Zhou L, Liu L, Chang L, Li L. Poisoning deaths in Central China (Hubei): a 10-year retrospective study of forensic autopsy cases. *J Forensic Sci* 2011;**56**(Suppl 1):S234–7.
- Jaekle RS, Nasrallah HA. Major depression and carbon monoxide-induced parkinsonism: diagnosis, computerized axial tomography, and response to L-dopa. *J Nerv Ment Dis* 1985;**173**:503–8.
- Kim JH, Chang KH, Song IC, Kim KH, Kwon BJ, Kim HC *et al*. Delayed encephalopathy of acute carbon monoxide intoxication: diffusivity of cerebral white matter lesions. *AJNR Am J Neuroradiol* 2003;**24**:1592–7.
- Hurley RA, Hopkins RO, Bigler ED, Taber KH. Applications of functional imaging to carbon monoxide poisoning. *J Neuropsych Clin Neurosci* 2001;**13**:157–60.
- Kao LW, Nanagas KA. Carbon monoxide poisoning. *Emerg Med Clin North Am* 2004;**22**:985–1018.
- Weaver LK, Hopkins RO, Chan KJ, Churchill S, Elliott CG, Clemmer TP *et al*. Hyperbaric oxygen for acute carbon monoxide poisoning. *N Engl J Med* 2002;**347**:1057–67.
- Weaver LK. Clinical practice. Carbon monoxide poisoning. *N Engl J Med* 2009;**360**:1217–25.
- Choi IS, Kim SK, Choi YC, Lee SS, Lee MS. Evaluation of outcome after acute carbon monoxide poisoning by brain CT. *J Korean Med Sci* 1993;**8**:78–83.
- Nabeshima T, Katoh A, Ishimaru H, Yoneda Y, Ogita K, Murase K *et al*. Carbon monoxide-induced delayed amnesia, delayed neuronal death and change in acetylcholine concentration in mice. *J Pharmacol Exp Ther* 1991;**256**:378–84.
- Thom SR. Carbon monoxide-mediated brain lipid peroxidation in the rat. *J Appl Physiol* 1990;**68**:997–1003.
- Thom SR, Bhopale VM, Fisher D, Zhang J, Gimotty P. Delayed neuropathology after carbon monoxide poisoning is immune-mediated. *Proc Natl Acad Sci USA* 2004;**101**:13660–5.
- Atalay H, Aybek H, Koseoglu M, Demir S, Erbay H, Bolaman AZ *et al*. The effects of amifostine and dexamethasone on brain tissue

- lipid peroxidation during oxygen treatment of carbon monoxide-poisoned rats. *Adv Ther* 2006;**23**:332–41.
- 13 Boylston M, Beer D. Methemoglobinemia: a case study. *Crit Care Nurse* 2002;**22**:50–5.
 - 14 Schirmer RH, Coulibaly B, Stich A, Scheiwein M, Merkle H, Eubel J *et al*. Methylene blue as an antimalarial agent. *Redox Rep* 2003;**8**:272–5.
 - 15 Meissner PE, Mandi G, Coulibaly B, Witte S, Tapsoba T, Mansmann U *et al*. Methylene blue for malaria in Africa: results from a dose-finding study in combination with chloroquine. *Malaria J* 2006;**5**:84.
 - 16 Oz M, Lorke DE, Petroianu GA. Methylene blue and Alzheimer's disease. *Biochem Pharmacol* 2009;**78**:927–32.
 - 17 Atamna H, Kumar R. Protective role of methylene blue in Alzheimer's disease via mitochondria and cytochrome c oxidase. *J Alzheimers Dis* 2010;**20**(Suppl 2):S439–52.
 - 18 Poteet E, Winters A, Yan LJ, Shufelt K, Green KN, Simpkins JW *et al*. Neuroprotective actions of methylene blue and its derivatives. *PLoS ONE* 2012;**7**:e48279.
 - 19 Ryou MG, Choudhury GR, Li W, Winters A, Yuan F, Liu R *et al*. Methylene blue-induced neuronal protective mechanism against hypoxia-reoxygenation stress. *Neuroscience* 2015;**301**:193–203.
 - 20 Wen Y, Li W, Poteet EC, Xie L, Tan C, Yan LJ *et al*. Alternative mitochondrial electron transfer as a novel strategy for neuroprotection. *J Biol Chem* 2011;**286**:16504–15.
 - 21 Roy Choudhury G, Winters A, Rich RM, Ryou MG, Gryczynski Z, Yuan F *et al*. Methylene blue protects astrocytes against glucose oxygen deprivation by improving cellular respiration. *PLoS ONE* 2015;**10**:e0123096.
 - 22 Lu Q, Tucker D, Dong Y, Zhao N, Zhang Q. Neuroprotective and functional improvement effects of methylene blue in global cerebral ischemia. *Mol Neurobiol* 2016;**53**:5344–55.
 - 23 Thom SR. Antagonism of carbon monoxide-mediated brain lipid peroxidation by hyperbaric oxygen. *Toxicol Appl Pharmacol* 1990;**105**:340–4.
 - 24 Thom SR. Dehydrogenase conversion to oxidase and lipid peroxidation in brain after carbon monoxide poisoning. *J Appl Physiol* 1992;**73**:1584–9.
 - 25 Thom SR, Bhopale VM, Fisher D. Hyperbaric oxygen reduces delayed immune-mediated neuropathology in experimental carbon monoxide toxicity. *Toxicol Appl Pharmacol* 2006;**213**:152–9.
 - 26 Zhang QG, Wang R, Khan M, Mahesh V, Brann DW. Role of Dickkopf-1, an antagonist of the Wnt/beta-catenin signaling pathway, in estrogen-induced neuroprotection and attenuation of tau phosphorylation. *J Neurosci* 2008;**28**:8430–41.
 - 27 Zhang QG, Wang R, Han D, Dong Y, Brann DW. Role of Rac1 GTPase in JNK signaling and delayed neuronal cell death following global cerebral ischemia. *Brain Res* 2009;**1265**:138–47.
 - 28 Lu Q, Rau TF, Harris V, Johnson M, Poulsen DJ, Black SM. Increased p38 mitogen-activated protein kinase signaling is involved in the oxidative stress associated with oxygen and glucose deprivation in neonatal hippocampal slice cultures. *Eur J Neurosci* 2011;**34**:1093–101.
 - 29 Han D, Scott EL, Dong Y, Raz L, Wang R, Zhang Q. Attenuation of mitochondrial and nuclear p38alpha signaling: a novel mechanism of estrogen neuroprotection in cerebral ischemia. *Mol Cell Endocrinol* 2015;**400**:21–31.
 - 30 Haan C, Behrmann I. A cost effective non-commercial ECL-solution for Western blot detections yielding strong signals and low background. *J Immunol Methods* 2007;**318**:11–9.
 - 31 Gan SD, Patel KR. Enzyme immunoassay and enzyme-linked immunosorbent assay. *J Invest Dermatol* 2013;**133**:e12.
 - 32 Barnes CA. Memory deficits associated with senescence: a neurophysiological and behavioral study in the rat. *J Comp Physiol Psychol* 1979;**93**:74–104.
 - 33 Ferguson SA, Law CD, Abshire JS. Developmental treatment with bisphenol A causes few alterations on measures of postweaning activity and learning. *Neurotoxicol Teratol* 2012;**34**:598–606.
 - 34 Alexis NE, Dietrich WD, Green EJ, Prado R, Watson BD. Nonocclusive common carotid artery thrombosis in the rat results in reversible sensorimotor and cognitive behavioral deficits. *Stroke* 1995;**26**:2338–46.
 - 35 Dowden J, Corbett D. Ischemic preconditioning in 18- to 20-month-old gerbils: long-term survival with functional outcome measures. *Stroke* 1999;**30**:1240–6.
 - 36 Plamondon H, Khan S. Characterization of anxiety and habituation profile following global ischemia in rats. *Physiol Behav* 2005;**84**:543–52.
 - 37 Nunn JA, LePeillet E, Netto CA, Hodges H, Gray JA, Meldrum BS. Global ischaemia: hippocampal pathology and spatial deficits in the water maze. *Behav Brain Res* 1994;**62**:41–54.
 - 38 Goodrich-Hunsaker NJ, Hunsaker MR, Kesner RP. The interactions and dissociations of the dorsal hippocampus subregions: how the dentate gyrus, CA3, and CA1 process spatial information. *Behav Neurosci* 2008;**122**:16–26.
 - 39 Danton GH, Dietrich WD. Inflammatory mechanisms after ischemia and stroke. *J Neuropathol Exp Neurol* 2003;**62**:127–36.
 - 40 Cao W, Carney JM, Duchon A, Floyd RA, Chevion M. Oxygen free radical involvement in ischemia and reperfusion injury to brain. *Neurosci Lett* 1988;**88**:233–8.
 - 41 Cadonic C, Sabbir MG, Albensi BC. Mechanisms of mitochondrial dysfunction in Alzheimer's disease. *Mol Neurobiol* 2016;**53**:6078–90.
 - 42 Bertholet AM, Delerue T, Millet AM, Moulis MF, David C, Daloyau M *et al*. Mitochondrial fusion/fission dynamics in neurodegeneration and neuronal plasticity. *Neurobiol Dis* 2016;**90**:3–19.
 - 43 Forni MF, Pelligia J, Trudeau K, Shirihai O, Kowaltowski AJ. Murine mesenchymal stem cell commitment to differentiation is regulated by mitochondrial dynamics. *Stem Cells* 2016;**34**:743–55.
 - 44 Jakobs S, Martini N, Schauss AC, Egner A, Westermann B, Hell SW. Spatial and temporal dynamics of budding yeast mitochondria lacking the division component Fis1p. *J Cell Sci* 2003;**116**(Pt 10):2005–14.
 - 45 Chen H, Detmer SA, Ewald AJ, Griffin EE, Fraser SE, Chan DC. Mitofusins Mfn1 and Mfn2 coordinately regulate mitochondrial fusion and are essential for embryonic development. *J Cell Biol* 2003;**160**:189–200.